Leveraging Inter-Layer Dependency for Post -Training Quantization

Anonymous Author(s)
Affiliation
Address
email

Abstract

Prior works on Post-training Quantization (PTQ) typically separate a neural network into sub-nets and quantize them sequentially. This process pays little attention to the dependency across the sub-nets, hence is less optimal. In this paper, we propose a novel Network-Wise Quantization (NWQ) approach to fully leveraging inter-layer dependency. NWQ faces a larger scale combinatorial optimization problem of discrete variables than in previous works, which raises two major challenges: over-fitting and discrete optimization problem. NWQ alleviates over fitting via a Activation Regularization (AR) technique, which better controls the activation distribution. To optimize discrete variables, NWQ introduces Annealing Softmax (ASoftmax) and Annealing Mixup (AMixup) to progressively transition quantized weights and activations from continuity to discretization, respectively. Extensive experiments demonstrates that NWQ outperforms prior state-of-the-art approaches by a large margin: 20.24% for the challenging configuration of MobileNetV2 with 2 bits on ImageNet, pushing extremely low-bit PTQ from feasibility to usability. In addition, NWQ is able to achieve competitive or better results with only 10% computation cost of previous works.

1 Introduction

Deep learning has seen a boom of architectures with ever-increasing capabilities and capacity. Huge capacity, however, always comes with boosting parameters, resulting in large computation cost and memory footprint. Researchers have utilized strategies like neural architecture search (NAS) [4, 11, 29, 50], network pruning [12, 19], and knowledge distillation (KD) [18, 21] to design compact networks and improve their accuracy. Furthermore, neural network quantization [7, 15, 22, 25, 28] is typically applied along with the methods mentioned above to reduce the computation cost and memory footprint. Quantization represents neural networks with lower bit precision, usually 8 bits in practice, and saves 75% of memory while offering $2 \sim 4\times$ speedup[26].

Network quantization techniques are typically categorized into Quantization Aware Training (QAT) and Post-training Quantization(PTQ) based on the dependency on labeled data and the necessity of weight tuning. Generally, PTQ techniques are preferred in industry because they rely less on labeled data and take into account privacy concerns as well as compute resources. This paper focuses on PTQ.

PTQ usually suffers from significant accuracy degradation, especially for low-bit quantization which offers much more memory reduction and speedup. To improve the accuracy of PTQ, much effort has been devoted [5, 32, 34, 36, 40]. AdaRound[32] has recently discovered that round-to-nearest appears to be optimal for single weight but not for the entire layer. The rounding errors of weights in a single layer have the capability of compensating for each other, contributing to a smaller layer-wise

Submitted to 36th Conference on Neural Information Processing Systems (NeurIPS 2022). Do not distribute.

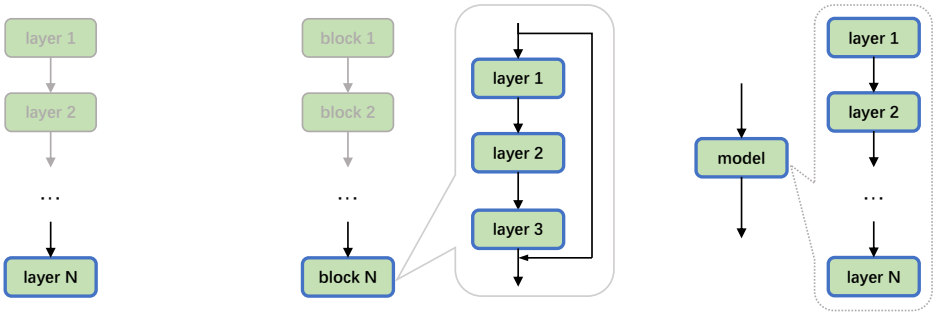

(a) layer-wise (b) block-wise (c) network-wise

Figure 1: **layer-wise vs. block-wise vs. network-wise**. Gray nodes are frozen while highlighted nodes are learnable (quantization parameters only). The term *block* here denotes residual unit in modern CNN (*e.g.* Residual Bottleneck for ResNets).

quantization error. We term this property as *intra-layer dependency*. Motivated by this property, AdaRound[32] proposes to learn the round policy layer by layer to improve accuracy.

Inspired by AdaRound[32], we hypothesize that the quantization errors of all layers in a network is able to compensate for each other, resulting in a reduced quantization error. We refer to this capability as *inter-layer dependency*. However, AdaRound assumes that layers are mutual-independent and derives a layer-diagonal Hessian, leading to a layer-wise solution(Figure 1a). BRECQ points out that the approximation of AdaRound is not accurate, they restrict the inter-layer dependency within a block and assume that blocks are mutual-independent, thus extend the Hessian to a block-diagonal matrix for a block-wise approach(Figure 1b). We argue that neither the approximations of AdaRound nor that of BRECQ are accurate enough, the inter-layer dependency should be leveraged in a network-wise manner. To achieve this, we propose a Network-Wise Quantization (NWQ, Figure 1c) scheme to fully leverage the inter-layer dependency. AdaRound and BRECQ separate a network into sub-nets and train them sequentially, this process makes the preceding layers unaware of succeeding layers. NWQ solves this problem via training the entire network end-to-end, where layers are aware of each other and they are able to cooperate for optimal solution. However, quantizing the entire network end-to-end is a combinatorial optimization problem where huge number of discrete parameters from all layers are combined together for optimization. This optimization problem will raise two major challenges that result in significant accuracy degradation.

The first challenge is over-fitting. Extending the reconstruction unit from layer/block to entire network will increase parameters dramatically and thus raises the risk of over-fitting over a typically small calibration set. To alleviate this issue, NWQ applies Activation Regularization (AR), a variant of L2 regularization, on intermediate representation to keep the quantized activations as close to the floating-point counterpart as possible. The benefits of AR are two folds. First, AR regularizes quantized activation flow to prevent over-fitting. Second, it works as a quantization loss function to encourage minimal intermediate quantization error. AR turns out to be both simple and effective.

Another challenge is discrete optimization. Based on AdaRound, NWQ learns the weight round policy and activation quantization parameters, both of which involve in discrete variables. However, the substantially increased depth and discrete variables make it more difficult to convergence compared to layer-wise[23, 32] and block-wise[27, 41] approach. The insufficient convergence will leave the discrete variables (weight round policy) in a state of continuity rather than discretization, leading to great performance drop. To solve this problem, we propose Annealing Sofmtax (ASoftmax) and Annealing Mixup (AMixup) to optimize discrete weights and activations via continuous relaxation [35]. Specifically, ASoftmax optimizes weight round policy via annealing the temperature to transition the continuous probability vector to one-hot vector. AMixup randomly mixes up the floating-point activations and the quantized counterpart and gradually decreasing the floating-point percentage. The benefit of ASoftmax and AMixup is that they guarantee the descretization after optimization while offering continuous relaxation.

Equipped with AR, ASoftmax and AMixup, we are able to build our NWQ framework that fully leverages *inter-layer dependency* to achieve higher accuracy than existing works.

To summarize, this paper makes the following contributions:

1. We propose a novel network-wise quantization framework for PTQ to fully leverage *inter-layer dependency*.
2. We analyze the combinatorial optimization problem introduced by network-wise quantization and propose AR, ASoftmax and AMixup to solve the over-fitting and discrete optimization problem.
3. We establish a new state-of-the-art through significantly improving PTQ by a large margin: 20.24% for MobileNetV2 with 2 bits and thus push the limit of extremely low-bit PTQ from feasibility to usability.

2 Related Work

Network quantization is commonly divided into QAT [7, 15, 22, 25, 49] and PTQ [27, 32, 33, 48]. QAT methods tend to minimize task error by training weights and quantization parameters jointly with the entire labeled dataset and thus require a large number of computing resources, whereas PTQ methods focus on finding optimal quantization parameters for off-the-shelf well-trained networks with much less data and compute resources than QAT. PTQ can further be classified into *statistic-based PTQ* and *learning-based PTQ*. Statistic-based PTQ methods [33, 36, 48] first estimate the distribution of activation on calibration data, and then find the optimal quantization parameters that minimize local quantization errors heuristically. Learning-based PTQ methods[23, 27, 32, 41] dedicate to slightly weight tuning and quantization parameters learning. Our work follows the learning-based PTQ scheme.

Learning-based PTQ: AdaRound[32] adopts the regime of learning the optimal round policy layer by layer. BRECQ [27] succeeds in extending AdaRound [32] to a block-wise reconstruction and concludes that block-wise quantization is superior to network-wise method. We argure that both layer-wise and block-wise approach is sub-optimal because the preceding layers/blocks are unaware of succeeding layers/block, thus the dependency they leveraged is unidirectional. Some works focus on the sequence of weight and activation quantization. AdaQuant [23] proposes to tune weights and activation quantization parameters separately for each layer to reduce over-fitting, while QDROP [41] finds that incorporating activation quantization into weight tuning can achieve higher accuracy.

Activiation Regularization: Large values in the learned dense representation can be a sign of being overfit. To encourage small activations, [31] employs L2 regularization on hidden state of recurrent neural networks (RNN), while various normalizations [2, 24, 39, 43] focus on centralize the activation distribution to regularize large values. Some prior works attempt to learn sparse representation. Dropout and its variants [1, 10, 37, 38, 42] randomly drop activations from the neural network to encourage sparsity. ReLUs[16, 20, 30, 44] dedicate to learning sparse representation via rectifying negative values. These techniques aim to regularize activations when training a neural network from scratch, which inapplicable for PTQ where the networks are off-the-shelf and well-trained, thus the activation distributions are deterministic and immutable. Instead of encouraging small and sparse activations, NWQ apply activation regularization on intermediate representation to encourage small offsets between quantized activations and the floating-point counterpart. AdaRound[32] and BRECQ [27] also employ quantization losses on intermediate activations but those losses works as optimization objectives rather than regularization, while objective of NWQ is to minimize the quantization error of the final network output and the regularization on intermediation activations is to prevent optmization process from over-fitting.

Discrete Optimization for Quantization: Network quantization optimizes discrete variables via gradient backpropagation. However, the quantization process introduces a round function which is indifferentiable. Some works on QAT focus on approximating the gradient through the round function [3, 6, 13, 14, 17, 45]. For PTQ, AdaRound [32] introduces additional discrete parameters(the binary round policy) and optimize them via Rectified Sigmoid with an explicit Regularization (RSeR) loss function. However, RSeR is adversarial to quantization loss and thus difficult to convergence in network-wise quantization. QDROP [41] proposes to randomly drop quantized activations to improve the flatness of optimization landscape, but introcues train-test inconsistency problem which results in performance degradation if used in network-wise PTQ.

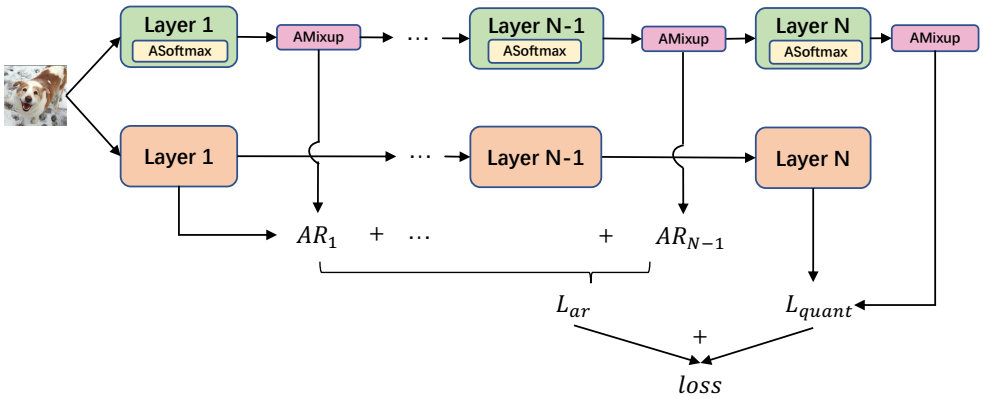

Figure 2: **Overfiew of NWQ**. We use L2 loss for both AR_i and L_{quant}. The green is simulated quantization network and the orange is the floating-point counterpart. We freeze all weights and train weight round policy and activation quantization parameters only.

3 Approach

Network-Wise Quantization (NWQ) is a simple end-to-end post-training quantization approach. The structure of NWQ is illustrated in Figure 2. The optimization objective is composed of output quantization loss and layer-wise AR loss. Meanwhile, the annealing approaches (Asoftmax and AMixup) are introduced in training process, which enable the quantized weights and activations to gently converge from continuous state to discrete state, lowering training complexity and improving accuracy.

3.1 Activation Regularization

NWQ leverages Activation Regularization (AR) to penalize quantized intermediate activations that are substantially away from the floating-point counterparts, thereby encouraging the activations to remain unchanged.

Formally, we define AR by:

$$L_{ar}(\overline{G}, G) = \sum_{l=1}^{N-1} \|\overline{a}_l - a_l\|_F^2, \tag{1}$$

while G represents floating-point network and $\overline{G}$ is the simulated quantized counterpart. a_l and $\overline{a}_l$ denote the floating-point and the simulated quantized activation of the l-th layer, respectively. N represents the number of total layers and $\|\cdot\|_F$ denotes the Frobenius norm. Our network quantization error $L_{quant}(\overline{a}_N, a_N)$ is defined by:

$$L_{quant}(\overline{G}, G) = \|\overline{a}_N - a_N\|_F^2,$$

then the final objective can be formulated as:

$$L(\overline{G}, G) = L_{ar} + L_{quant} = \sum_{l=1}^{N} \|\overline{a}_l - a_l\|_F^2. \tag{2}$$

Practically, L_{ar} is not restricted to be utilized layer by layer, it can also be performed block by block and stage by stage, as BRECQ [27] defined. We will discuss how the granularity affects the performance in Sec. 4.2.1. By default, we employ layer-wise AR in our experiments.

3.2 Annealing Softmax

For a weight vector $\mathbf{w}$, AdaRound [32] proposes to learn the round policy by:

$$\hat{\mathbf{w}}_i = clip\left(\lfloor \frac{\mathbf{w}_i}{s} \rfloor + h(\mathbf{v}_i), q_-, q_+\right), \tag{3}$$

where $\lfloor \cdot \rfloor$ gives as output of the integral part and $clip(\cdot)$ clamps all values between q_- and q_+. $\hat{\mathbf{w}}_i$ denotes the quantized weight for the i-th element of $\mathbf{w}$. We will omit i below for simplicity. s is the quantizer step size. $\mathbf{v}$ is a learnable continuous vector *w.r.t.* $\mathbf{w}$ and $h(\mathbf{v})$ is *recitified sigmoid* function (see Eqn.(4)) which is regularized to converge to $\{0, 1\}$.

$$h(\mathbf{v}) = clip(\frac{1.2}{1 + exp(-\mathbf{v})} - 0.1, 0, 1). \tag{4}$$

Based on Eqn.(4), AdaRound proposes Rectified Sigmoid with an explicit Regularization (RSeR) to discrete $h(\mathbf{v})$:

$$L_{RSeR}(h(\mathbf{v})) = 1 - |2h(\mathbf{v}) - 1|^{\beta}, \tag{5}$$

However, there are two limitations of RSeR. First, RSeR works only for binary round policy. Second, RSeR is adversarial to quantization loss. For example, for a linear transformation network, the quantization loss is

$$\begin{aligned} L_q &= \|\mathbf{w}^\intercal \mathbf{x} - s\hat{\mathbf{w}}^\intercal \mathbf{x}\|_F^2 \\ &= \|(\frac{\mathbf{w}}{s} - \lfloor \frac{\mathbf{w}}{s} \rfloor - h(\mathbf{v}))^\intercal \mathbf{x}\|_F^2, \end{aligned} \tag{6}$$

where $\mathbf{x}$ denotes the input and we ignore the *clip* function in Eqn. (3).

Eqn. (6) indicates that quantization loss will prevent L_{RSeR} from convergence (*i.e.*, L_{RSeR} encourages $h(\mathbf{v})$ to binary while L_q prefers $\frac{\mathbf{w}}{s} - \lfloor \frac{\mathbf{w}}{s} \rfloor$). Besides, this adversarial become more severe when extending layer/block-wise methods to network-wise quantization(see Sec. 4.2.2 and Table 4).

3.2.1 Formulation

To resolve the two problems of RSeR, we propose Annealing Softmax (ASoftmax). First, we extend the discrete optimization space of $h(\cdot)$ from $\{0, 1\}$ to $\mathcal{K}$, where $\mathcal{K}$ is a integer range and defined by:

$$\mathcal{K} = \{n, n+1, ..., m-1, m\}, n \in \mathbb{Z}_{\leq 0}, m \in \mathbb{Z}_{>0}, \tag{7}$$

where n and m are hyper-parameters that specify the discrete optimization space. Then, ASoftmax can be formulated as:

$$\hat{\mathbf{w}}^t = clip\left(\lfloor \frac{\mathbf{w}}{s} \rfloor + h^t(\mathbf{V}), q_-, q_+\right), \tag{8}$$

where $\mathbf{V}$ is a continuous learnable matrix and represents the logits of probability over $\mathcal{K}$. $h^t(\mathbf{V})$ is defined by:

$$h^t(\mathbf{V}) = \mathbb{E}_{k \sim p(k|\mathbf{V}, \tau^t)}\Big[k\Big], \tag{9}$$

$$p(k = \mathcal{K}_i | \mathbf{V}, \tau^t) \propto exp(\mathbf{V}_i / \tau^t), 0 \leq i < m - n + 1, \tag{10}$$

where t represents for t-th iteration. τ^t is a temperature that decays linearly to transition $h^t(\mathbf{V})$ from continuity to discretization. For example, when τ^t is large, $p(k|\mathbf{V}, \tau^t)$ is a continuous vector of probability and $h^t(\mathbf{V})$ is the $expectation$ of the discretization. When τ^t turns tiny, $p(k|\mathbf{V}, \tau^t)$ becomes a one-hot vector and $h^t(\mathbf{V})$ selects k by $p(k|\mathbf{V}, \tau^t) = 1$. τ^t is simply decayed by:

$$\tau^t = \frac{(\tau^T - \tau^0) \cdot t}{T} + \tau^0, \tag{11}$$

where τ^0 and τ^T are hyper-parameters of initial and final temperature.

ASoftmax is a general formation of learning wider range of discrete parameters than binary. It easily degenerates to round policy learning by setting $n = 0$ and $m = 1$. We use $\tau^T = 0.01$ and $\tau^0 = 1$ by default.

3.2.2 Initialization

According to our observations, initialization has significant impacts on learning round policy. Given the weight quantizer step size s, which has been computed using statistic-based PTQ methods, we attempt to initialize $\mathbf{V}$ in order to make $s \cdot \hat{\mathbf{w}}^0$ as close to floating-point $\mathbf{w}$ as possible at the start. To achieve this goal, we first calculate the un-normalized probability by:

$$\sigma'(\mathbf{V})_i = \frac{1}{|\mathcal{K}_i - (\frac{w}{s} - \lfloor \frac{w}{s} \rfloor)|}, 0 \leq i < m - n + 1. \tag{12}$$

Then, we normalize the probability:

$$\sigma(\mathbf{V})_i = \frac{\sigma'(\mathbf{V})_i}{\sum_{k=0}^{m-n} \sigma'(\mathbf{V})_k}, \tag{13}$$

Finally, the initialization for $\mathbf{V}_i$ is $log(\sigma(\mathbf{V})_i)$. It can be easily proved (see Appendix A) that the initialized $s \cdot \hat{\mathbf{w}}^0$ equals $\mathbf{w}$ as long as the integer range $\mathcal{K}$ is symmetric *w.r.t.* 0.5 (*i.e.* $n = 1 - m$).

3.3 Annealing Mixup

NWQ considers activation quantization as a discrete optimization problem and solves it via continuous relaxation. Different from ASoftmax which is applied on element-wise level, AMixup works on tensor-wise level: we randomly mix up the floating-point activations with the simulated quantized activations. To encourage continuous relaxation converge to discretization, NWQ progressively decreases the percentage of floating-point activations, so the mixed activations will become fully quantized activation gradually.

Formally, the percentage of floating-point activations is defined by:

$$P(t) = \frac{(P_e - P_s) \cdot t}{T} + P_s, \tag{14}$$

where $P(t)$ is the percentage of floating-point activation in the mixed activation for the t-th iteration. P_s and P_e denote the percentage at start and end respectively, and T is the number of iterations. We use $P_s = 0.5$ and $P_e = 0$ by default.

AMixup is similar to QDROP [41] in the mixup operation. The key difference, however, is that AMixup introduces an annealing process. This is very important for NWQ. QDROP trains with mixed activations while testing with fully quantized activations, thus introducing inconsistency bias. This bias accmulates as network depth increases and leads to great accuracy degradation in network-wise quantization. AMixup is able to eliminate the inconsistency bias via the annealing process.

4 Experiments

In this section, we conduct extensive experiments with various architectures to verify our NWQ. We first compare our method with previous state-of-the-art, and then we delve into our important designs and fully explore the scalability, effectiveness, and efficiency of our solution. We report top-1 classification accuracy on the ImageNet[9] validation set.

Implementation Details. Our code is based on open-source codes BRECQ and QDrop. We apply layer-wise AR. For ASoftmax, we set $n = 0, m = 1$ and τ is decayed from 1 to 0.01. For AMixup, we set default P_s as 0.5 and P_e as 0. We randomly sample 1024 images from ImageNet train set and employ Cutmix [46] and Mixup[47] as data augmentation. The learning rates are 0.01 for round policy and 0.0004 for activation quantizer step size. We train for 20000 iterations with a mini-batch size of 32 in 8 Tesla V100 GPUs, taking $\sim$ 30 minutes for ResNet18, which is on par with BRECQ and QDROP. Our experiments are conducted on 5 architectures, including ResNet18(Res18), MobileNetV2(MNV2), RegNet-600MF(Reg600MF), RegNet-3.2GF(Reg3.2GF) nad MnasNet(Mnas). Other settings remain same as QDROP[41] if not specified. We use above hyper-parameters across the entire paper by default unless explicitly specified.

4.1 Comprehensive Comparison

Table 1 compares our NWQ with several main-stream PTQ approaches. Overall, NWQ outperforms previous works across all neural network architectures and bit widths, and our performance improves even more as the bit width decreases.

Classicial Calibration Set. Following previous works, we compare the performance on a small calibration set of 1024 images. For start, we achieve 0.2%$\sim$ 0.9% improvement even compared with strong baselines on W4A4, which are rather close to full precision accuracy. For W3A3, NWQ yields 0.83%$\sim$ 3.26% and reduces the gap between W3A3 and W4A4. For the challenging W2A2, our method surpasses the previous state-of-the-art by a large margin of 13.37% for MobileNetV2 and 12.4% for MnasNet, pushing the limit of extremely low-bit PTQ step further.

	Bits(W/A)	Res18	MobileNetV2	Reg600MF	Reg3.2GF	MnasNet2.0
Full Prec	32/32	71.06	72.49	73.71	78.36	76.68
ACIQ-Mix* [36]	4/4	67.00	-	-	-	-
ZeroQ* [5]	4/4	21.71	26.24	28.54	12.24	3.89
LAPQ* [34]	4/4	60.30	49.70	57.71	55.89	65.32
AdaQuant* [23]	4/4	69.60	47.16	-	-	-
Bit-Split* [40]	4/4	67.56	-	-	-	-
AdaRound* [32]	4/4	67.96	61.52	68.20	73.85	68.86
BRECQ* [27]	4/4	69.60	66.57	68.33	74.21	73.56
QDROP* [41]	4/4	69.62	68.84	71.18	76.66	73.71
QDROP† [41]	4/4	69.88	69.15	71.45	77.02	74.09
NWQ(Ours)	4/4	69.85±0.04	69.14±0.12	71.92±0.07	77.40±0.04	74.60±0.09
NWQ†(Ours)	4/4	**69.95**±0.07	**69.60**±0.03	**72.03**±0.09	**77.42**±0.03	**74.86**±0.03
AdaQuant* [23]	3/3	60.09	2.23	-	-	-
AdaRound* [32]	3/3	64.66	15.20	51.01	56.79	47.89
BRECQ* [27]	3/3	65.87	23.41	55.16	57.12	49.78
QDROP* [41]	3/3	66.75	57.98	65.54	72.51	66.81
QDROP† [41]	3/3	67.51	58.54	66.75	73.48	68.28
NWQ(Ours)	3/3	67.58±0.14	61.24±0.21	67.38±0.13	74.79±0.09	68.85±0.18
NWQ†(Ours)	3/3	**68.15**±0.10	**62.53**±0.05	**68.31**±0.09	**75.44**±0.08	**70.77**±0.10
BRECQ* [27]	2/2	42.54	0.24	3.58	3.62	0.61
QDROP* [41]	2/2	54.72	13.05	41.47	55.11	28.77
QDROP† [41]	2/2	57.84	14.89	45.93	57.98	34.19
NWQ(Ours)	2/2	59.14±0.05	26.42±1.03	48.49±0.03	62.85±0.13	41.17±0.35
NWQ†(Ours)	2/2	**61.65**±0.12	**35.13**±2.16	**56.36**±0.01	**67.02**±0.01	**53.55**±0.20

Table 1: **Comprehensive comparison**. We report top1 accuracy on the ImageNet validation set. $*$ represents for reference from QDROP[41] and † means scaling up the calibration set to 10240 images. QDROP† results are produced by open-source codes from QDrop. We use $n = 0, m = 1$ for NWQ and $n = -1, m = 2$ for NWQ†. We follow BRECQ[27] to set the first and the last layer to 8-bit.

Scaled-up Calibration Set. To further explore the potential of NWQ, we scale up the calibration set by $10\times$ and reproduce QDROP on the scaled-up calibration set, building a very strong baseline. Interestingly, NWQ outperforms QDROP even with one-tenth data. When equipping NWQ with the scaled-up calibration set, we observe significant improvement under all settings. Particularly, the accuracy gaps of W2A2 between NWQ and QDROP are enlarged even more as the calibration set scales up. For example, the gap of MnasNet increases from 12.4% to 19.36%, and that of MobileNetV2 increases from 13.37% to 20.24%, showing the excellent scalability of our method.

4.2 Ablation Study

4.2.1 AR

The Effect of AR. We study the effect of AR via comparing the experiments with layer-wise AR to the experiments without AR on W2A2. Table 2 shows that layer-wise AR improves the accuracy significantly. It's worth noting that layer-wise AR improves 5.22% for MobileNetV2 and 10.42% for MnasNet. To understand how AR works, we analyze the loss curves during training in Figure 3. First, our AR experiment consistently converges to lower loss on both the train and test datasets, resulting in higher accuracy. Second, AR accelerates convergence significantly and thus allows NWQ to reach competitive accuracy at a substantially lower computing cost. Third, even though AR does not totally eliminate over-fitting, it effectively bridges the loss gap between train and test datasets.

The Effect of Granularity. Table 2 studies how AR granularity affects accuracy. We discover that lightweight networks prefer coarse-grained AR, whereas heavyweight networks prefer fine-grained AR. MobileNetV2, RegNet-600MF, and MnasNet, for example, achieve the best performance with block-wise AR, whereas ResNet18 and RegNet-3.2GF achieve the maximum accuracy with layer-wise AR.

Comparison with Data Augmentation. Data augmentation is a classical strategy used to relieve over-fitting due to its simplicity and effectiveness. We compare AR with strong augmentation (*e.g.*

Granularity	Res18	MNV2	Reg600M	Reg3.2G	Mnas
layer-wise AR	**59.14**	26.42	48.49	**62.85**	41.17
block-wise AR	59.12	**26.52**	**48.89**	61.31	**41.89**
stage-wise AR	59.10	25.52	47.28	60.30	41.25
w/o AR	57.94	21.20	46.82	59.82	30.75

Table 2: **AR *vs.* w/o AR** on W2A2 with our NWQ approach. Up: Comparison of different AR granularities. Bottom: Experiments without AR. The definition of granularity refers to BRECQ[27].

AR	AA	Res18	MNV2	Reg600M	Reg3.2G	Mnas
✗	✗	57.94	21.20	46.82	59.82	30.75
✗	✓	58.99	24.86	47.92	62.19	38.16
✓	✗	59.14	26.42	48.49	62.85	41.17
✓	✓	**59.52**	**26.90**	**48.62**	**63.52**	**42.92**

Table 3: **AR *vs.* AutoAugment** on W2A2. For AutoAugment, we use the open-source codes from torchvision. AA is short for AutoAugment.

Method	RSeR						ASoftmax
LW	0.01	0.1	1	10	100	1000	-
Res18	0.96	3.49	34.75	**46.56**	44.54	43.83	**59.14**
MNV2	0.10	0.11	0.28	0.87	**4.86**	2.95	**26.42**

Table 4: **ASoftmax *vs.* RSeR** on W2A2 with our NWQ approach. *LW* represents the regularization loss weight for AdaRound. We simply replace ASoftmax with RSeR in our NWQ solution.

Initialization	Bits(W/A)	ResNet18	MobileNetV2
random	2/2	55.33	22.00
Ours	2/2	**59.14**	**26.42**

Table 5: Comparison of different initialization methods. We compare random initialization with our method described in Sec. 3.2.2.

AutoAugment[8]) in Table 3. Notably, both AR and AutoAugment significantly improve accuracy, with AR contributing more than AutoAugment, particularly for sparse networks like MobileNetV2 and MnasNet. Coupling these two techniques enables us to achieve better performance.

4.2.2 ASoftmax Study

The Effect of ASoftmax. Table 4 compares ASoftmax to Rectified Sigmoid with explicit Regularization (RSeR) which is used in AdaRound. We simply replace ASoftmax with RSeR in our NWQ and run a grid search on regularization loss weight to explore the potential of RSeR. We discover that RSeR requires a huge loss weight for NWQ, which is $10^3 \sim 10^5\times$ larger than that of subnet-wise approaches. Even with exhausting hyper-parameter search, RSeR does not perform as well as in the subnet-wise method. ASoftmax, on the other hand, outperforms RSeR by 12.58% and 21.56% on ResNet18 and MobileNetV2, respectively, without any additional hyper-parameter tuning.

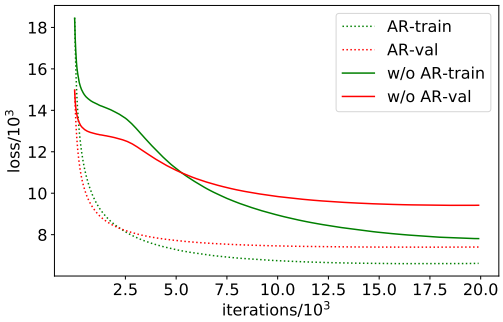

Figure 3: **AR *vs.* w/o AR.** Quantization loss curves on calibration set of 1024 images and validation set of 5×10^4 images. Experiments are performed on MobileNetV2 with W2A2 for 2×10^4 iterations.

The Effect of Initialization. Table 5 demonstrates the effectiveness of our initialization, which keeps the quantization model close to the float-point at the start to steady the training.

The Robustness of τ. We investigate the robustness of τ in Table 6. τ starts with a large number to encourage continuous relaxation and ends with a small value to favor one-hot distribution. The final τ^T determines the decaying speed of τ. It can be observed that τ^T has a robustness range of $10^{-2} \sim 10^{-4}$, making it easily adaptable to a wider range of neural network architectures.

The Extensiveness of ASoftmax. As described in Sec. 3.2.1, ASoftmax can easily extend the discrete parameter space from $\{0, 1\}$ to a larger integer range, offering the opportunity for a better optimum. However, extending discrete range benefits MobileNetV2 and RegNet-600MF while degrading RegNet-3.2GF on a small calibration set, as shown in Table 7 upper group. We argue that the enlarged discrete range raises the risk of over-fitting for large networks. When we scale up the calibration set, the performance no longer degrades and the performance improves even more.

τ^T	Res18	MNV2	Reg600M	Reg3.2G	Mnas
1e-1	59.08	12.19	47.84	60.10	33.92
1e-2	**59.14**	26.42	48.49	**62.85**	41.17
1e-3	59.05	**26.75**	**49.77**	62.09	**41.34**
1e-4	58.98	24.74	49.42	62.06	41.32

Table 6: **Robustness of τ^T for ASoftmax** on W2A2. Experiments are conducted with $\tau^0 = 1.0$

#Images	n/m	Res18	MNV2	Reg600M	Reg3.2G	Mnas
1024	0/1	59.14	26.42	48.49	62.85	41.17
1024	-1/2	59.10	28.73	49.73	61.68	41.07
10240	0/1	61.61	29.54	53.83	67.02	51.15
10240	-1/2	**61.65**	**35.13**	**56.36**	**67.02**	**53.55**

Table 7: **Extensiveness of ASoftmax** on W2A2. MNV2 is short for MobileNetV2.

Method	Bits(W/A)	ResNet18	MobileNetV2
w/o Drop	2/2	58.42	25.09
QDROP-style	2/2	56.47	5.13
AMixup	2/2	**59.12**	**26.42**

Table 8: **w/o Drop *vs.* QDROP-style *vs.* AMixup** on W2A2 with our NWQ approach. Effect of different dropping methods coupled with NWQ. w/o Drop represnets for training without dropping or mixup operation.

P_s	Res18	MNV2	Reg600M	Reg3.2G	Mnas
1	**59.47**	25.34	**50.53**	**63.06**	40.55
0.8	59.39	25.57	50.05	62.65	40.66
0.6	59.32	24.18	49.84	61.90	40.86
0.5	59.14	**26.42**	48.49	62.85	**41.17**
0.4	59.08	25.79	48.83	61.73	40.63
0.2	58.96	25.44	48.81	60.76	39.71

Table 9: **Decay Policy of AMixup** on W2A2. We use $P_e = 0$ for all of the experiments.

4.2.3 AMixup Study

The Effect of AMixup. QDROP presents good performance in block-wise reconstruction, but fails in our network-wise scheme. As illustrated in Table 8, we achieve 1.95% improvement for ResNet18 and 19.96% for MobileNetV2 by simply removing QDROP. We hypothesize that randomly mixing activations up introduces inconsistency bias between the training and test phase, which is concealed by the improvement of flatness in block-wise reconstruction. However, as the reconstruction unit goes deeper (from block to network) and sparser, the problem becomes more pronounced, resulting in significant degeneration. Over-parameterized ResNet18 is able to compensate for the side effect, but MobileNetV2 suffers a great performance drop. Remarkably, our AMixup is able to overcome the inconsistency while taking advantage of the flatness, contributing to higher accuracy.

The Policy of Decay. Table 9 explores the influence of different decay policies. We run a grid search for P_s while freezing P_e as 0. It's worth noting that MobileNetV2 and MnasNet prefer 0.5, whereas ResNet18 and RegNet prefer 1. The basic law is very similar to that of AR granularity, which states that heavyweight networks require more regularization, implying that AMixup and AR are both capable of regularizing accuracy.

4.3 Efficiency

We compare the efficiency of several approaches on ResNet18. According to Figure 4, NWQ outperforms QDROP and BRECQ under various iterations. Specifically, NWQ achieve competitive results only 10% computation cost, demonstrating the efficiency of NWQ. As the number of iterations increases, NWQ continues to improve accuracy, whereas BRECQ and QDROP reach their saturation at $\sim 1.6 \times 10^4$ iterations.

5 Discussion and Conclusion

Simple algorithms that scale well are the core of deep learning. Prior works tend to quantize networks in layer-wise and block-wise manner. We prove that network-wise quantization is a simpler and more effective way than layer/block-wise solutions. To accomplish this, we analyze the problems introduced by the network-wise regime and propose three key designs to address them. Based on that, we construct a simple and effective end-to-end network-wise PTQ framework. Extensive experiments demonstrate that our solution is scalable, effective, and efficient. However, there is still a large accuracy gap between low-bit PTQ and full precision network, and we believe that there is still much room for further improvement for PTQ, which is a key direction for future research.

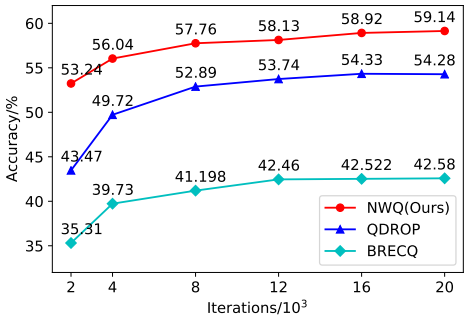

Figure 4: **Accuracy *w.r.t.* iterations**. The experiments are conducted on ResNet18 with W2A2.

Broder impacts. The proposed method uses GPU resources for training, thus resulting in a certain amount of energy consumption and carbon footprints. For example, it takes about 4 GPU-hours for our method to quantize ResNet18, which would consume around 1 kWh and produce around 1 lbs of CO2, accelerating climate change and global warming in some degree.

References

[1] Jimmy Ba and Brendan Frey. Adaptive dropout for training deep neural networks. *Advances in neural information processing systems*, 26, 2013.

[2] Jimmy Lei Ba, Jamie Ryan Kiros, and Geoffrey E Hinton. Layer normalization. *arXiv preprint arXiv:1607.06450*, 2016.

[3] Yu Bai, Yu-Xiang Wang, and Edo Liberty. Proxquant: Quantized neural networks via proximal operators. *arXiv preprint arXiv:1810.00861*, 2018.

[4] Han Cai, Chuang Gan, Tianzhe Wang, Zhekai Zhang, and Song Han. Once-for-all: Train one network and specialize it for efficient deployment. In *International Conference on Learning Representations*, 2019.

[5] Yaohui Cai, Zhewei Yao, Zhen Dong, Amir Gholami, Michael W Mahoney, and Kurt Keutzer. Zeroq: A novel zero shot quantization framework. In *Proceedings of the IEEE/CVF Conference on Computer Vision and Pattern Recognition*, pages 13169–13178, 2020.

[6] Shangyu Chen, Wenya Wang, and Sinno Jialin Pan. Metaquant: Learning to quantize by learning to penetrate non-differentiable quantization. *Advances in Neural Information Processing Systems*, 32, 2019.

[7] Matthieu Courbariaux, Yoshua Bengio, and Jean-Pierre David. Training deep neural networks with low precision multiplications. *arXiv preprint arXiv:1412.7024*, 2014.

[8] Ekin D Cubuk, Barret Zoph, Dandelion Mane, Vijay Vasudevan, and Quoc V Le. Autoaugment: Learning augmentation policies from data. *arXiv preprint arXiv:1805.09501*, 2018.

[9] Jia Deng, Wei Dong, Richard Socher, Li-Jia Li, Kai Li, and Li Fei-Fei. Imagenet: A large-scale hierarchical image database. In *2009 IEEE conference on computer vision and pattern recognition*, pages 248–255. Ieee, 2009.

[10] Terrance DeVries and Graham W Taylor. Improved regularization of convolutional neural networks with cutout. *arXiv preprint arXiv:1708.04552*, 2017.

[11] Xuanyi Dong, Lu Liu, Katarzyna Musial, and Bogdan Gabrys. NATS-Bench: Benchmarking nas algorithms for architecture topology and size. *IEEE Transactions on Pattern Analysis and Machine Intelligence (TPAMI)*, 2021. doi:10.1109/TPAMI.2021.3054824.

[12] Xuanyi Dong and Yi Yang. Network pruning via transformable architecture search. In *The Conference on Neural Information Processing Systems (NeurIPS)*, pages 760–771, 2019.

[13] Zhen Dong, Zhewei Yao, Daiyaan Arfeen, Amir Gholami, Michael W Mahoney, and Kurt Keutzer. Hawq-v2: Hessian aware trace-weighted quantization of neural networks. *Advances in neural information processing systems*, 33:18518–18529, 2020.

[14] Zhen Dong, Zhewei Yao, Amir Gholami, Michael W Mahoney, and Kurt Keutzer. Hawq: Hessian aware quantization of neural networks with mixed-precision. In *Proceedings of the IEEE/CVF International Conference on Computer Vision*, pages 293–302, 2019.

[15] Steven K Esser, Jeffrey L McKinstry, Deepika Bablani, Rathinakumar Appuswamy, and Dharmendra S Modha. Learned step size quantization. In *International Conference on Learning Representations*, 2019.

[16] Xavier Glorot, Antoine Bordes, and Yoshua Bengio. Deep sparse rectifier neural networks. In *Proceedings of the fourteenth international conference on artificial intelligence and statistics*, pages 315–323. JMLR Workshop and Conference Proceedings, 2011.

[17] Ruihao Gong, Xianglong Liu, Shenghu Jiang, Tianxiang Li, Peng Hu, Jiazhen Lin, Fengwei Yu, and Junjie Yan. Differentiable soft quantization: Bridging full-precision and low-bit neural networks. In *Proceedings of the IEEE/CVF International Conference on Computer Vision*, pages 4852–4861, 2019.

[18] Shaopeng Guo, Yujie Wang, Quanquan Li, and Junjie Yan. Dmcp: Differentiable markov channel pruning for neural networks. In *Proceedings of the IEEE/CVF Conference on Computer Vision and Pattern Recognition (CVPR)*, June 2020.

[19] Song Han, Huizi Mao, and William J Dally. Deep compression: Compressing deep neural networks with pruning, trained quantization and huffman coding. *International Conference on Learning Representations (ICLR)*, 2016.

[20] Kaiming He, Xiangyu Zhang, Shaoqing Ren, and Jian Sun. Delving deep into rectifiers: Surpassing human-level performance on imagenet classification. In *Proceedings of the IEEE international conference on computer vision*, pages 1026–1034, 2015.

[21] Geoffrey Hinton, Oriol Vinyals, and Jeffrey Dean. Distilling the knowledge in a neural network. In *NIPS Deep Learning and Representation Learning Workshop*, 2015.

[22] Itay Hubara, Matthieu Courbariaux, Daniel Soudry, Ran El-Yaniv, and Yoshua Bengio. Quantized neural networks: Training neural networks with low precision weights and activations. *The Journal of Machine Learning Research*, 18(1):6869–6898, 2017.

[23] Itay Hubara, Yury Nahshan, Yair Hanani, Ron Banner, and Daniel Soudry. Improving post training neural quantization: Layer-wise calibration and integer programming. *arXiv preprint arXiv:2006.10518*, 2020.

[24] Sergey Ioffe and Christian Szegedy. Batch normalization: Accelerating deep network training by reducing internal covariate shift. In *International conference on machine learning*, pages 448–456. PMLR, 2015.

[25] Benoit Jacob, Skirmantas Kligys, Bo Chen, Menglong Zhu, Matthew Tang, Andrew Howard, Hartwig Adam, and Dmitry Kalenichenko. Quantization and training of neural networks for efficient integer-arithmetic-only inference. In *Proceedings of the IEEE conference on computer vision and pattern recognition*, pages 2704–2713, 2018.

[26] Raghu Krishnamoorthi. QUANTIZATION IN PYTORCH. https://slidetodoc.com/quantization-in-pytorch-raghu-krishnamoorthi-facebook-quantization-n/, 2019. [Online; accessed 19-May-2022].

[27] Yuhang Li, Ruihao Gong, Xu Tan, Yang Yang, Peng Hu, Qi Zhang, Fengwei Yu, Wei Wang, and Shi Gu. Brecq: Pushing the limit of post-training quantization by block reconstruction. *arXiv preprint arXiv:2102.05426*, 2021.

[28] Darryl Lin, Sachin Talathi, and Sreekanth Annapureddy. Fixed point quantization of deep convolutional networks. In *International conference on machine learning*, pages 2849–2858. PMLR, 2016.

[29] Hanxiao Liu, Karen Simonyan, and Yiming Yang. Darts: Differentiable architecture search. In *International Conference on Learning Representations*, 2018.

[30] Andrew L Maas, Awni Y Hannun, Andrew Y Ng, et al. Rectifier nonlinearities improve neural network acoustic models. In *Proc. icml*, volume 30, page 3. Citeseer, 2013.

[31] Stephen Merity, Bryan McCann, and Richard Socher. Revisiting activation regularization for language rnns. *arXiv preprint arXiv:1708.01009*, 2017.

[32] Markus Nagel, Rana Ali Amjad, Mart Van Baalen, Christos Louizos, and Tijmen Blankevoort. Up or down? adaptive rounding for post-training quantization. In *International Conference on Machine Learning*, pages 7197–7206. PMLR, 2020.

[33] Markus Nagel, Mart van Baalen, Tijmen Blankevoort, and Max Welling. Data-free quantization through weight equalization and bias correction. In *Proceedings of the IEEE/CVF International Conference on Computer Vision*, pages 1325–1334, 2019.

[34] Yury Nahshan, Brian Chmiel, Chaim Baskin, Evgenii Zheltonozhskii, Ron Banner, Alex M Bronstein, and Avi Mendelson. Loss aware post-training quantization. *Machine Learning*, 110(11):3245–3262, 2021.

[35] Panos M Pardalos. Continuous approaches to discrete optimization problems. In *Nonlinear optimization and applications*, pages 313–325. Springer, 1996.

[36] B Ron, J Perera, E Hoffer, and D Soudry. Aciq: Analytical clipping for integer quantization of neural networks. *arXiv preprint arXiv:1810.05723*, 2018.

[37] Nitish Srivastava, Geoffrey Hinton, Alex Krizhevsky, Ilya Sutskever, and Ruslan Salakhutdinov. Dropout: a simple way to prevent neural networks from overfitting. *The journal of machine learning research*, 15(1):1929–1958, 2014.

[38] Jonathan Tompson, Ross Goroshin, Arjun Jain, Yann LeCun, and Christoph Bregler. Efficient object localization using convolutional networks. In *Proceedings of the IEEE conference on computer vision and pattern recognition*, pages 648–656, 2015.

[39] Dmitry Ulyanov, Andrea Vedaldi, and Victor Lempitsky. Instance normalization: The missing ingredient for fast stylization. *arXiv preprint arXiv:1607.08022*, 2016.

[40] Peisong Wang, Qiang Chen, Xiangyu He, and Jian Cheng. Towards accurate post-training network quantization via bit-split and stitching. In *International Conference on Machine Learning*, pages 9847–9856. PMLR, 2020.

[41] Xiuying Wei, Ruihao Gong, Yuhang Li, Xianglong Liu, and Fengwei Yu. Qdrop: Randomly dropping quantization for extremely low-bit post-training quantization. *arXiv preprint arXiv:2203.05740*, 2022.

[42] Haibing Wu and Xiaodong Gu. Max-pooling dropout for regularization of convolutional neural networks. In *International Conference on Neural Information Processing*, pages 46–54. Springer, 2015.

[43] Yuxin Wu and Kaiming He. Group normalization. In *Proceedings of the European conference on computer vision (ECCV)*, pages 3–19, 2018.

[44] Bing Xu, Naiyan Wang, Tianqi Chen, and Mu Li. Empirical evaluation of rectified activations in convolutional network. *arXiv preprint arXiv:1505.00853*, 2015.

[45] Jiwei Yang, Xu Shen, Jun Xing, Xinmei Tian, Houqiang Li, Bing Deng, Jianqiang Huang, and Xian-sheng Hua. Quantization networks. In *Proceedings of the IEEE/CVF Conference on Computer Vision and Pattern Recognition*, pages 7308–7316, 2019.

[46] Sangdoo Yun, Dongyoon Han, Seong Joon Oh, Sanghyuk Chun, Junsuk Choe, and Youngjoon Yoo. Cutmix: Regularization strategy to train strong classifiers with localizable features. In *Proceedings of the IEEE/CVF international conference on computer vision*, pages 6023–6032, 2019.

[47] Hongyi Zhang, Moustapha Cisse, Yann N Dauphin, and David Lopez-Paz. mixup: Beyond empirical risk minimization. *arXiv preprint arXiv:1710.09412*, 2017.

[48] Ritchie Zhao, Yuwei Hu, Jordan Dotzel, Chris De Sa, and Zhiru Zhang. Improving neural network quantization without retraining using outlier channel splitting. In *International conference on machine learning*, pages 7543–7552. PMLR, 2019.

[49] Shuchang Zhou, Yuxin Wu, Zekun Ni, Xinyu Zhou, He Wen, and Yuheng Zou. Dorefa-net: Training low bitwidth convolutional neural networks with low bitwidth gradients. *arXiv preprint arXiv:1606.06160*, 2016.

[50] Barret Zoph and Quoc V Le. Neural architecture search with reinforcement learning. *arXiv preprint arXiv:1611.01578*, 2016.

Checklist

1. For all authors...
   (a) Do the main claims made in the abstract and introduction accurately reflect the paper's contributions and scope? [Yes]
   (b) Did you describe the limitations of your work? [Yes]
   (c) Did you discuss any potential negative societal impacts of your work? [Yes] See broader impacts.
   (d) Have you read the ethics review guidelines and ensured that your paper conforms to them? [Yes]
2. If you are including theoretical results...
   (a) Did you state the full set of assumptions of all theoretical results? [Yes]
   (b) Did you include complete proofs of all theoretical results? [Yes]
3. If you ran experiments...
   (a) Did you include the code, data, and instructions needed to reproduce the main experimental results (either in the supplemental material or as a URL)? [Yes]
   (b) Did you specify all the training details (e.g., data splits, hyperparameters, how they were chosen)? [Yes]
   (c) Did you report error bars (e.g., with respect to the random seed after running experiments multiple times)? [Yes] We report error bars in Table 1.
   (d) Did you include the total amount of compute and the type of resources used (e.g., type of GPUs, internal cluster, or cloud provider)? [Yes]

4. If you are using existing assets (e.g., code, data, models) or curating/releasing new assets...
   (a) If your work uses existing assets, did you cite the creators? [Yes]
   (b) Did you mention the license of the assets? [Yes]
   (c) Did you include any new assets either in the supplemental material or as a URL? [No]
   (d) Did you discuss whether and how consent was obtained from people whose data you're using/curating? [No]
   (e) Did you discuss whether the data you are using/curating contains personally identifiable information or offensive content? [No] We use public datasets only.
5. If you used crowdsourcing or conducted research with human subjects...
   (a) Did you include the full text of instructions given to participants and screenshots, if applicable? [N/A]
   (b) Did you describe any potential participant risks, with links to Institutional Review Board (IRB) approvals, if applicable? [N/A]
   (c) Did you include the estimated hourly wage paid to participants and the total amount spent on participant compensation? [N/A]

A ASoftmax Initialization

First of all, We define the fractional part of x as: $\{x\} = x - \lfloor x \rfloor$, and we use $\overline{\mathbf{w}}^0$ to represent initially simulated quantization of $\mathbf{w}$. According to equation (9),(10), (12) and (13), we get:

$$
\begin{aligned}
h^0(\mathbf{V}) &= \mathbb{E}_{k\sim p(\mathcal{K}_i|\mathbf{V},\tau^t)}\Big[k\Big] \\
&= \sum_{i=0}^{m-n} \mathcal{K}_i * \sigma^0(\mathbf{V})_i \\
&= \frac{1}{\sum_{i=0}^{m-n}\hat{\sigma}^0(\mathbf{V})_i}\sum_{i=0}^{m-n} \mathcal{K}_i * \hat{\sigma}^0(\mathbf{V})_i \\
&= \frac{1}{\sum_{i=0}^{m-n}\hat{\sigma}^0(\mathbf{V})_i}\sum_{i=0}^{-n} \Big(\mathcal{K}_i * \hat{\sigma}^0(\mathbf{v})_i + (1-\mathcal{K}_i) * \hat{\sigma}^0(\mathbf{v})_{m-n-i}\Big) \\
&= \frac{1}{\sum_{i=0}^{m-n}\hat{\sigma}^0(\mathbf{V})_i}\sum_{i=0}^{-n} \left(\frac{\mathcal{K}_i}{\{\frac{w}{s}\}-\mathcal{K}_i} + \frac{1-\mathcal{K}_i}{1-\mathcal{K}_i-\{\frac{w}{s}\}}\right) \\
&= \frac{1}{\sum_{i=0}^{m-n}\hat{\sigma}^0(\mathbf{V})_i}\sum_{i=0}^{-n} \left(\frac{(1-2\mathcal{K}_i)\{\frac{w}{s}\}}{(\{\frac{w}{s}\}-\mathcal{K}_i)(1-\mathcal{K}_i-\{\frac{w}{s}\})}\right) \\
&= \frac{\{\frac{w}{s}\}}{\sum_{i=0}^{m-n}\hat{\sigma}^0(\mathbf{V})_i}\sum_{i=0}^{-n} \left(\frac{1-2\mathcal{K}_i}{(\{\frac{w}{s}\}-\mathcal{K}_i)(1-\mathcal{K}_i-\{\frac{w}{s}\})}\right) \\
&= \frac{\{\frac{w}{s}\}}{\sum_{i=0}^{m-n}\hat{\sigma}^0(\mathbf{V})_i}\sum_{i=0}^{-n} \left(\frac{1}{\{\frac{w}{s}\}-\mathcal{K}_i} + \frac{1}{1-\mathcal{K}_i-\{\frac{w}{s}\}}\right) \\
&= \frac{\{\frac{w}{s}\}}{\sum_{i=0}^{m-n}\hat{\sigma}^0(\mathbf{V})_i}\sum_{i=0}^{m-n} \hat{\sigma}^0(\mathbf{V})_i \\
&= \{\frac{w}{s}\}
\end{aligned}
\tag{15}
$$

If we disregard the $clip$ function, then

$$
\begin{aligned}
\overline{\mathbf{w}}^0 &= \hat{\mathbf{w}}^0 \cdot s \\
&= (\lfloor \frac{\mathbf{w}}{s} \rfloor + h^0(\mathbf{V})) \cdot s \\
&= (\lfloor \frac{\mathbf{w}}{s} \rfloor + \{\frac{\mathbf{w}}{s}\}) \cdot s \\
&= \frac{\mathbf{w}}{s} \cdot s \\
&= \mathbf{w}
\end{aligned}
\tag{16}
$$